

Investigation of Quantum Phase Transitions using Multi-target DMRG Methods

C. Degli Esposti Boschi^{a,†}

F. Ortolani^{a,b,‡}

^a *Unità di ricerca INFN di Bologna,*

^{a,b} *Dipartimento di Fisica, Università di Bologna and INFN,
viale Berti-Pichat, 6/2, 40127, Bologna, Italia*

[†] `desposti@bo.infm.it`

[‡] `ortolani@bo.infn.it`

June 20, 2019

Abstract

In this paper we examine how the predictions of conformal invariance can be widely exploited to overcome the difficulties of the density-matrix renormalization group near quantum critical points. The main idea is to match the full spectrum of low-lying energy levels of the lattice Hamiltonian, as a function of the system's size, with the one expected for a given conformal field theory in two dimensions. Hence a trustable method to target various excited states at once is needed. We discuss how this can be achieved within the DMRG algorithm by means of the so-called Thick-restart Lanczos method. As a nontrivial benchmark we use an anisotropic spin-1 Hamiltonian with special attention to the transitions from the Haldane phase. Nonetheless, the ideas presented here can have a general validity in the study of quantum critical phenomena.

PACS: 75.40.Mg Numerical simulation studies, 05.10.Cc Renormalization group methods, 75.10.Pq Spin chain models.

1 Outline and General Facts

The density-matrix renormalization group (DMRG) was invented by S. R. White in the early 90's and nowadays is recognized as one of the most accurate and efficient numerical techniques in the study of correlated quantum systems [1]. A number of authors is still contributing to its development for new applications and one of the major points is the dimensionality of the system. While for 1D lattices of spins or electrons there exist several firm results, a generally accepted DMRG scheme in 2D is still lacking despite the numerous proposals. However, even for 1D systems, it is known that the DMRG encounters some difficulties in reproducing the physics of quantum critical points. This is because one wants, at the same time, to explore larger and larger system's sizes and to maintain a good numerical precision in order to locate the points where the excitation gap closes and to compute the associated critical exponents. If the quantum chain has q states per site, the dimension of the full Hilbert space for L sites grows exponentially as q^L . The main (and smart) approximation of the DMRG is the truncation to the space spanned by the M eigenvectors of the block density matrix,

ρ_b , corresponding to the M largest eigenvalues (weights). The problem is that, close to criticality, the system experiences fluctuations on very large scales and (as will be discussed in sec. 4) the spectrum of ρ_b decays more slowly than in noncritical cases. Hence if one considers, as a first indicator of the accuracy of the method, the sum of the discarded weights $W_M = \sum_{j>M} w_j$, then this different decay implies that the minimal M to go below a prescribed threshold is generally larger when the system is close to a critical point. To be more specific, Legeza and co-workers [2, 3] found that the error on the ground state (GS) energy due to a finite M , at a fixed L , is simply:

$$\delta E_L^{\text{GS}}(M) = E_L^{\text{GS}}(M) - E_L^{\text{GS}}(\infty) \propto W_M \quad (1)$$

Now, if we admit that the precision on the first excited state follows a similar trend, then there will be a regime, close to the critical point and/or for large L (see sec. 2), where W_M becomes larger than the excitation gap itself. In addition, figs. 3 and 5 of ref. [2] indicate two other important features (at least for the Ising model in transverse field). First, at criticality the error on the energy at fixed M increases appreciably with the chain's length, and again we see that fixing M once for all while taking larger and larger values of L is not a completely safe procedure. The second, and more important point is that the proportionality in eq. (1) holds only after that a few *finite-system* iterations are performed. Using Legeza's terms, these are necessary to cancel the so-called environment error that dominates at sufficiently small L . The crossover from the environment-dominated regime to the truncation-dominated one is marked by a characteristic size, $L^*(M)$, which increases with increasing M . In sec. 5 we will argue that a similar characteristic length emerges in critical spin-1 chains too. Finally, in our opinion, the result of Andersson, Boman & Östlund [4] regarding a critical chain of free spinless fermions, or equivalently a spin-1/2 XX model, point somehow in the same direction. Even if the system is known to be rigorously critical, the effect of a finite number of DMRG states is to introduce a *fake correlation length*, that grows as $M^{1.3}$.

We believe that the considerations above indicate that the critical behaviour of (1D) quantum systems cannot be "simply" approached by using the computational resources to reach larger and larger values of L by means of the infinite-system DMRG, as it is sometimes done (see, for instance, [5] and refs. therein). Rather, we prefer to exploit as much as possible the consequences of *conformal invariance*. On general grounds, indeed, we expect that the low-energy physics of a 1D quantum system near its critical points is described by a suitable conformal field theory (CFT) in (1+1) dimensions. Qualitatively, this is because the path integral formulation of a D -dimensional quantum problem can be made equivalent to the partition function of a $(D+1)$ -dimensional classical system, where the time (either continuous or discretized [6]) plays the role of the extra dimension. For integrable systems the connection can be made at the lattice level, identifying the quantum Hamiltonian, H , with the logarithmic derivative of a classical transfer matrix (see, among others, [7, 8, 9] and quoted refs.) Then, if the (1+1) classical system is to be critical, we imagine that there will be a scale-invariant effective continuum model that captures its universal features. In 2D the key point is that all these universality classes are encompassed in the framework of CFT's. In the last twenty years the numerous exact results in this area have been organized into an elegant framework, which is however too vast for our purposes. Therefore, in sec. 2 we sketch only the points of contact with our analysis and refer to [10] for a comprehensive guide and to [11] for a shorter review on finite-size effects.

2 Identification of the CFT through the Finite-Size Spectrum

The requirement of scale invariance in 2D is sufficiently strong to allow (under general assumptions) a classification of the states of a quantum field theory in terms of the irreducible representations of the Virasoro algebra generated by a set of operators satisfying:

$$[L_m, L_n] = (m - n)L_{m+n} + \frac{c}{12}\delta_{m+n,0}(m^3 - m), \quad m, n \in \mathbb{Z} \quad (2)$$

(As customary in CFT, the statements and equations regarding the holomorphic part should always be suitably repeated for the antiholomorphic part, denoted by overbars). For unitary theories the central charge of the algebra is either $c \geq 1$, or can be chosen as one of the values $c = 1 - 6/p(p+1)$ ($p = 2, 3, \dots$), each one corresponding to a so-called minimal model. In the latter case, once a $c < 1$ is given, one can decompose the Hilbert space into a *finite* number of irreducible representations of (2) labeled by the eigenvalues of the generator L_0 :

$$L_0|\Delta\rangle = \Delta|\Delta\rangle, \quad \Delta = \frac{[(p+1)r - ps]^2 - 1}{4p(p+1)}, \quad 1 \leq s \leq r \leq p-1 \in \mathbb{Z}. \quad (3)$$

More specifically, the states $|\Delta\rangle$ are annihilated by L_m with positive m and are obtained from the vacuum, $|\text{vac}\rangle$, by applying the so-called primary fields Φ_Δ . Each of these ones generates its own conformal family, $[\Phi_\Delta]$, that contains all the states obtained through the application of the negative-integer generators $|\Delta\rangle_m^k = (L_{-m})^k|\Delta\rangle = (L_{-m})^k\Phi_\Delta|\text{vac}\rangle$ (the secondary or descendant states and fields - taking care of null vectors). It can be seen, as a consequence of the Virasoro algebra, that these are in turn eigenvectors of L_0 :

$$L_0|\Delta\rangle_m^k = (\Delta + mk)|\Delta\rangle_m^k. \quad (4)$$

In principle, all the correlation functions of the fields of the theory can be reduced to correlators of primary fields. Moreover, the operators L_0, \bar{L}_0 play a special role as can be seen by considering a conformal transformation that map the plane onto an infinite cylinder, whose circumference of length L represents the space axis (with periodic boundary conditions). Then the energy and momentum operators are simply expressed as:

$$H_{\text{CFT}} = \frac{2\pi v}{L} \left[L_0 + \bar{L}_0 - \frac{c}{12} \right], \quad Q = \frac{2\pi}{L} [L_0 - \bar{L}_0]. \quad (5)$$

Actually, the prefactor v has been inserted “by hand” in view of the identification of the (critical part of the) spectrum of the original quantum Hamiltonian with the values predicted by the CFT construction. More specifically, the GS is simply identified with $|\text{vac}\rangle$, for which both L_0 and \bar{L}_0 have null eigenvalues. Thus, the finite-size corrections to vacuum energy are:

$$E_L^{\text{vac}} = -\frac{\pi c v}{6L}, \quad (6)$$

whereas the excited states follow from the construction after eq. (3):

$$E_L(\Delta, m, k; \bar{\Delta}, \bar{m}, \bar{k}) - E_L^{\text{GS}} = \frac{2\pi v}{L} [\Delta + \bar{\Delta} + mk + \bar{m}\bar{k}]. \quad (7)$$

It is important to recall that the sum of the eigenvalues of L_0 and \bar{L}_0 , that is the last term in square brackets of eq. (7), is called the *scaling dimension* because it enters the algebraic decay of the correlation function of the corresponding field:

$$\langle O(0,0)O(z,\bar{z}) \rangle \sim z^{-2(\Delta+mk)} \bar{z}^{-2(\bar{\Delta}+\bar{m}\bar{k})} \Big|_{z=\bar{z}=r} = r^{-2d_O},$$

$$O(z, \bar{z}) \equiv (\bar{L}_{-m})^{\bar{k}} \bar{\Phi}_{\bar{\Delta}}(\bar{z})(L_{-m})^k \Phi_{\Delta}(z) \ , \ d_O = \Delta + \bar{\Delta} + mk + \bar{m}\bar{k} \ , \quad (8)$$

where the last equality in the first line comes from the calculation at time 0, so that $z = \bar{z} = r$. In the language of renormalization group (RG) theory, the operators are seen to be relevant when $d_O < 2$, irrelevant when $d_O > 2$ and marginal when the scaling dimension is exactly 2 (in 2D). The exponents, y_i , of the scaling fields near a fixed point of the RG flow are simply given by $y_i = 2 - d_i$. Eqs. (4), (7) and (8) generalize to more complicated secondary operators obtained from the composition of various Virasoro generators with different m .

The edge case $c = 1$ opens the way to unitary CFT's with an infinite number of primary fields. It is related to certain topological constructions of a free bosonic field [12], and the operators (or the associated states) are furtherly classified in terms of an $\hat{U}(1)$ Kac-Moody algebra. Here we won't enter into more details since ref. [13] is specifically devoted to the study of such $c = 1$ CFT's starting from the spin-1 defined by eq. (13), using just the method explained in the present paper.

Finally, the case $c > 1$ contains both *rational* and *irrational* CFT's and the the complexity of the problem in its generality simply forbids us a further explanation within this context. We will content ourselves with the observation that, at least for the former case, the algebraic structure of the theories can often be understood in terms of irreducible representations of higher algebras into which one can organize the infinite representations of the Virasoro one. At least from an operative point of view, the equations above should remain valid once that the labels $\Delta, \bar{\Delta}$ and the secondary indices are properly interpreted in terms of the wider algebra, that has to be investigated case by case.

The first problem is, of course, that one does not know, *a priori*, which is the CFT that has to be invoked. A great step towards the answer to this question is made if one knows the so-called *central charge* of the theory, c , that characterizes the underlying Virasoro algebra (2). Apart from the algebra itself and the operator product expansion of the stress-energy tensor, the central charge appears explicitly in the size-dependence of the GS energy density:

$$\frac{E_L^{\text{GS}}}{L} = \epsilon_{\infty} - \frac{\pi c v}{6L^2} \ . \quad (9)$$

which is nothing but eq. (6) plus an infinite-size term, which is absent in the formal CFT but has a definite value for a given quantum Hamiltonian.

In quantum field theory the second term of (9) accounts for the Casimir effect [14], while in statistical systems it gives the correction to the free energy at small temperatures (L playing the role of $1/T$ [15]). In our case, eq. (9) is the starting point to discover the CFT that is appropriate for the problem under consideration. Indeed, having good estimates of E_L^{GS} at various L , we can first best-fit ϵ_{∞} and cv . Then, if we have reasons to believe that one of the states has scaling dimension 1 [eqs. (7) and (8)], then we can calculate also:

$$v = \frac{\Delta E_L(d=1)}{2\pi/L} \ . \quad (10)$$

If we now interpret $\Delta k = 2\pi/L$ as the quantum of momentum for a chain of length L , then eq. (10) looks as a discrete derivative of the energy vs momentum relation, that is, a group velocity. This somehow explains the term "spin velocity", which is widely used in the literature of quantum spin chains independently of the real nature of the excitations that correspond to $\Delta E(d=1)$ (see examples below).

Summing up, with a combined usage of eqs. (9) and (10) we can calculate c from the numerical data of the first excited levels at different chain's lengths. Then the identification may fall into two cases. For $c < 1$, unitarity demands that the values of the central charge are quantized, according to the list of minimal models. In this case, a small discrepancy from one of these values is likely to be related to

numerical uncertainties. The matter becomes more complicated when one finds a numerical c larger than one, in which case unitarity by itself is not sufficient to provide a quantization condition. The symmetries of the lattice Hamiltonian in this second case are of great help because we expect them to be present also in the corresponding continuum model. Then one may focus on the known 2D field theories whose actions are invariant under both this symmetry group and under conformal transformations. From an operative point of view, an approach like that of Tsai and Marston [16], based on finite-size analysis of certain observables in the middle of the chain obtained through the infinite-system algorithm (and with open boundary conditions), may prove to be very useful to get a first insight into the underlying CFT and the associated critical exponents. Nonetheless, we discourage a blind usage of the infinite-system DMRG to conclude (as in ref. [5]) that the numerical discrepancies from the expected values are to be ascribed to nontrivial effects beyond the CFT framework. In doubt, the final answer should always come from a careful refinement using *finite-system* numerical data, in a range of L where the scaling behaviour is visible but the accuracy is not corrupted significantly by the DMRG truncation error.

In any case, what we are actually doing is a self-consistent guess of the underlying CFT. In principle, this allows an analytical calculation of the scaling dimensions, d_ℓ of all the operators associated with the excited states. The corresponding energy gaps, here formally indexed by ℓ , scale according to eq. (7):

$$\Delta E_L^\ell = \frac{2\pi}{L} v d_\ell. \quad (11)$$

Matching the numerical spectrum of a certain number of levels with the structure encoded in the scaling dimensions of eq. (11) represents a particularly stringent test of the hypothesis above. Eventually, it is useful to see also how this expression changes when when a term $(g - g_c) \int V$ is added to the continuum Hamiltonian. At first order in perturbation theory Cardy finds [17, 18]:

$$\Delta E_L^\ell = \frac{2\pi v}{L} [d_\ell + C^\ell (g - g_c) L^{2-d_V} + \dots], \quad (12)$$

where d_V is the scaling dimension of the perturbing operator V and C^ℓ is a constant proportional to the prefactors appearing in the operator product expansion of V with the operator associated with the ℓ -th state.

3 Model and Details of the Implementation: Multi-target Method

Following our previous paper [13] we have considered the following spin-1 Hamiltonian:

$$H = \sum_j \left[\frac{1}{2} (S_j^+ S_{j+1}^- + S_j^- S_{j+1}^+) + \lambda S_j^z S_{j+1}^z + D (S_j^z)^2 \right] \quad (13)$$

for a chain of L spins which includes both an Ising-like and a single-ion anisotropy term, with coefficients λ and D respectively. Formally we have set $\hbar = 1$ and the overall coupling constant $J = 1$ so that every quantity turn out to be dimensionless and we have imposed periodic boundary (PBC) conditions: $\mathbf{S}_{j+L} = \mathbf{S}_j \quad \forall j = 1, \dots, L$. See [19, 20, 21, 22, 13] for a discussion of the various phases in the λ - D diagram.

The algorithm that we have implemented for DMRG calculations follows rather closely the lines indicated by White in his seminal papers [23, 24]. As regards our specific application, we should outline the following points.

The superblock geometry was chosen to be $[\mathbf{B}^r \bullet |\mathbf{B}_{\text{ref}}^{r'} \bullet]$ with PBC, where $\mathbf{B}_{\text{ref}}^{r'}$ is the (left \leftrightarrow right) reflected of block $\mathbf{B}^{r'}$ with r' sites. The rationale for adopting this

configuration is that, being effectively on a ring, the two blocks are always separated by a single site, for which the operators are small matrices that are treated exactly (no truncation) [24]. In this way we expect a better precision in the correlation functions calculated fixing one of the two point on these sites and moving the other one along the block. Moreover, whenever the system has an imposed antiferromagnetic structure (typically when a staggered field is switched on), this geometry seems to be the one that preserve it at best, both for even and odd values of r . In a recent application of the DMRG to quantum chemistry calculations [3] it has been pointed out that the configuration of the superblock may be one of the major points of optimization of the method for future applications. As regards the choice of the boundary conditions, we are aware of the fact that with open conditions a smaller M is generally required and that in certain cases (i.e. Gaussian transitions) the introduction of twisted boundary conditions is a clever trick to identify the critical point using numerical data on relatively small systems [18, 25, 26, 22]. Nevertheless, in our set of calculations we have adopted PBC to get rid of the edge effects that in some cases mask almost all the informations contained in very short-ranged (string) correlation functions. Moreover, we are primarily interested in the transtions from the Haldane phase, for which it is known that the finite-size GS acquires a fourfold degeneracy due to the two free effective spins at the ends of the chain [27]. With PBC instead, one has a unique finite-size GS so that the convergence of the Lanczos procedure is better and the analysis of the numerical is simpler.

We used the finite-system algorithm with three iterations. This prescription should ensure the virtual elimination of the so-called environment error [2], which is expected to dominate in the very first iterations for $L < L^*(M)$ (see below). In fact, it is only after a suitable number of such sweeps that we may expect that the error on the energies has been minimized (for given L and M) and eq. (1) holds true. Normally the correlations are computed at the end of the third iteration, once that the best approximation of the GS is available.

Dealing with quantum spin chains, we always exploit the conservation of the z -component of the total spin, M^z . For problems of correlated electrons, this corresponds to exploring the spectrum at various numbers of particles. Typically we are interesred in nonmagnetic GS's, that is, with $M^z = 0$. In every studied case the correlations have been calculated targeting only the lowest-energy state within this sector. However, in order to analyse the energy spectrum, we had to target the lowest-energy state(s) in the other sectors $|M^z| = 1, 2, \dots$ and/or target also a few excited states within the $M^z = 0$ sector, depending on the phase under study. The standard Lanczos algorithm gives with enough precision the ground state of the system, but it is not so accurate for the excited states. Moreover, as a consequence of a general theorem on tridiagonal symmetric matrices, we can't have degenerate states from this method. So it is required to modify the algorithm to allow the building of the reduced density matrix over the block as a mixture of the matrices corresponding to each target state. While for the latter point we are not aware of any specific "recipe" other than that of equal weights, the implementation of the multi-target diagonalization routine within our DMRG code is based on the so-called Thick Restart Lanczos method of Wu and Simon [28].

Once M^z is fixed, in a given run we wish to follow simultaneously the first levels $|M^z; \mathbf{b}\rangle$ with $\mathbf{b}=0,1,2,\dots,t$ [the GS being identified by $(M^z = 0, \mathbf{b}= 0)$]. Then, as in the conventional Lanczos scheme, we have to iterate until the norms of the residual vectors and/or the differences of the energies in consecutive steps are smaller than prescribed tolerances ($10^{-9} - 10^{-12}$ in our calculations). The delicate point to keep under control is that, once the lowest state $|M^z; 0\rangle$ is found, if we keep iterating searching for higher levels the orthogonality of the basis may be lost, just because the eigenvectors corresponding to these levels tend to overlap again with the vector $|M^z; 0\rangle$. As a result, the procedure is computationally more demanding to the extent that one

has to re-orthogonalize the basis from time to time. We have seen that this part takes a 10-20% of the total time spent in each call to the Lanczos routine. We have also observed that if this re-orthogonalization is not performed, one of the undesired effects is that the excited doublets (typically due to momentum degeneracy) are not computed correctly. More specifically, it seems that while the two energy values are nearly the same in the asymmetric stages of the sweeps, when the superblock geometry becomes symmetric ($r = r'$ in the notations of the preceding point) the double degeneracy is suddenly lost in a spurious way. This is line with the results of ref. [3], where the error on the energy is kept under control by means of a dynamically-adjusted M and the configurations that require a larger number of DMRG states are just those near the symmetric one.

4 Dependence on the Number of DMRG States

As discussed in the introduction of sec. 1 the choice of the number of optimized states with respect to the chain length L is the crucial point to address in any DMRG calculation. Being conscious that the energy accuracy is *not* an exhaustive indicator, from eq. (1) one should try, at least, to keep the discarded weight W_M as small as possible. This quantity, in turn, is related to the decay of the density matrix eigenvalues $\{w_j\}$ as a function of the index j :

$$W_M = \sum_{j>M} w_j = \sum_j D_j z_j, \quad (14)$$

where the last equality is a simple rewriting in terms of the degeneracies D_j and of the distinct eigenvalues z_j . The issue appeared to be quite important from the very beginning and is the core of the success of the DMRG. In [24, 29] it was argued that the convergence of the GS energy of a gapped or a spatially finite system is roughly exponential in M :

$$\delta E_L \propto e^{-M/M^*(L)}, \quad (15)$$

with a superimposed step-like behaviour, probably related to the successive inclusion of more and more complete spin sectors. It is also generally believed that this exponential decay becomes slower (possibly algebraic) when a critical point is approached. At this stage it is interesting to recall that for integrable systems the spectrum of ρ_b can be determined exactly. In fact, it can be seen [8] that for a quantum chain the infinite- L block density matrix is given by $\rho_b = \chi^4$, where χ is the corner transfer matrix of the associated 2D classical statistical system. This statement has a wide generality, with the exception of critical cases where the boundary effects may have some role and are expected to affect the tails of the distribution [30]. For integrable systems a further step can be made: χ is expressed as the exponential of a pseudo-Hamiltonian, K , that involves the same local operators of the Hamiltonian (e.g. $\vec{S}_j \cdot \vec{S}_{j+1}$) but with coefficients depending on the site index j . Moreover, the spectrum of K can be determined exactly and, typically, the eigenvalues turn out to be equally spaced. Therefore the distinct eigenvalues of ρ_b decay as:

$$z_j \propto Z^j, \quad Z = e^{-\epsilon}, \quad (16)$$

$\epsilon/4$ being the level spacing of $-K$. These predictions have been explicitly verified for the Ising model in transverse field [8] and for the XXZ spin-1/2 Heisenberg chain [8, 9].

Now we shall try to elucidate this topic in the case of critical spin-1 systems using the Hamiltonian of eq. (13). At ($\lambda = 1, D = 0$) one has an isotropic antiferromagnetic (AF) Heisenberg chain of integer spin, whose theoretical interest comes from what is now known as Haldane's conjecture [31], that predicts a genuine quantum behaviour with a finite energy gap in the excitation spectrum. This has to be contrasted with

what happens in half-odd-integer cases that are gapless (i.e. critical) in the thermodynamic limit (TL), $L \rightarrow \infty$. Another important theoretical contribution is the mapping between spin chains and restricted solid-on-solid models proposed by den Nijs and Rommelse [32]. Qualitatively, the Haldane phase is interpreted as a spin-liquid, in the sense that the effective particles - $|0\rangle$ means an empty site and $|\pm\rangle$ represent a particle with spin up or down - are positionally disordered but carry antiferromagnetic order. In the quantum states that contribute to the GS, this order is hidden by arbitrarily long strings of $|0\rangle$'s but can be measured by the so-called string order parameters [32, 27]:

$$O_S^\alpha \equiv \lim_{|j-k| \rightarrow \infty} O_S^\alpha(j, k) \quad (17)$$

$$O_S^\alpha(j, k) \equiv - \left\langle S_j^\alpha \exp \left(i\pi \sum_{n=j+1}^{k-1} S_n^\alpha \right) S_k^\alpha \right\rangle, \quad (18)$$

the expectation value being taken on the GS.

Beside that, nowadays there exist several experimental realizations of these anisotropic spin-1 chains: to the author's knowledge, RbNiCl_3 and Y_2BaNiO_5 are examples of pure Haldane systems, CsNiFe_3 is a ferromagnet ($\lambda = -1$) with appreciable single-ion anisotropy ($D \simeq 0.4$) and $\text{CoCl}_2 \cdot 2 \text{H}_2\text{O}$ behaves as an Ising ferromagnet ($|\lambda| \gg 1$) with high easy-axis anisotropy ($D \simeq -5$). The so-called NENP and NENC represent, respectively, small- D ($\simeq 0.16$) and large- D ($\simeq 7.5$) antiferromagnets with easy-plane anisotropy.

In order to study the convergence of truncation errors close to criticality we have selected a pair of representative points in the phase diagram. In the origin ($\lambda = 0, D = 0$), where a Berezinskii-Kosterlitz-Thouless (BKT) transition is expected [33], we have the spin-1 analogue of the XX spin-1/2 case used in ref. [4] to examine the effect of a finite M on a quantum critical system. The second point that we examine in this section is ($\lambda = 1, D = 0.95$) because from refs. [13, 26] we know that it lies very close to the line of transition from the Haldane phase to the so-called large- D phase. In the following numerical analysis these two points will be denoted by XX and H-D, respectively. The results can be thought as the critical counterpart of the ones presented in [9] for an isotropic spin-1 Heisenberg chain.

For the H-D point we have computed the first excited state in the sectors with $M^z = 0, 1$ for $L = 16, 20, 24, 32, 48$ and 64 , using $M = 81, 162, 243, 324$ and 405 DMRG states for each case. For the XX point, we have monitored the same states for the same values of M using also $L = 28$. The exponential decay of eq. (15) seems to be appropriate in all the cases, as shown in the examples of fig. 1. For every fixed L we best-fit the energy-vs- M data and read off the characteristic values $M^*(L)$, represented in fig. 2. Of course, the larger is L the larger is M^* , and it seems that the curves do not saturate indicating, as reasonable, that a finite M is not sufficient to describe properly a (quasi-)critical system with arbitrarily large L . However, the promising feature of fig. 2 is that the various data sets approximately lie in a strip of the $m - \ln L$ plot, characterized by a linear slope $M_0 = 15 \pm 3$. More precisely, this value is an overall measure of the slopes of the best-fit straight lines, reported in table 1 for the six sets considered. In other terms, if we invert the relation between M and L , we find $L^*(M) \propto \exp(M/M_0)$, that means that for fixed M we expect a good convergence of the energies for $L < L^*(M)$ (negligible truncation error, in the language of [2]) and that the gain in increasing M is exponential with a surprisingly small reference value M_0 (in line with the first observations of White himself [24]). Interestingly enough, the logarithmic behaviour of $M^*(L)$ can be justified by taking eq. (16) to be valid even at critical points. There one expects $\epsilon \rightarrow 0$ and indeed conformal invariance indicates that the finite-size level spacing vanishes as $\epsilon = \epsilon_0 / \ln L$ (with ϵ_0 a constant) [8]. Now, if we approximate the discarded weight of eq. (14) ignoring the degeneracy factor D_j ,

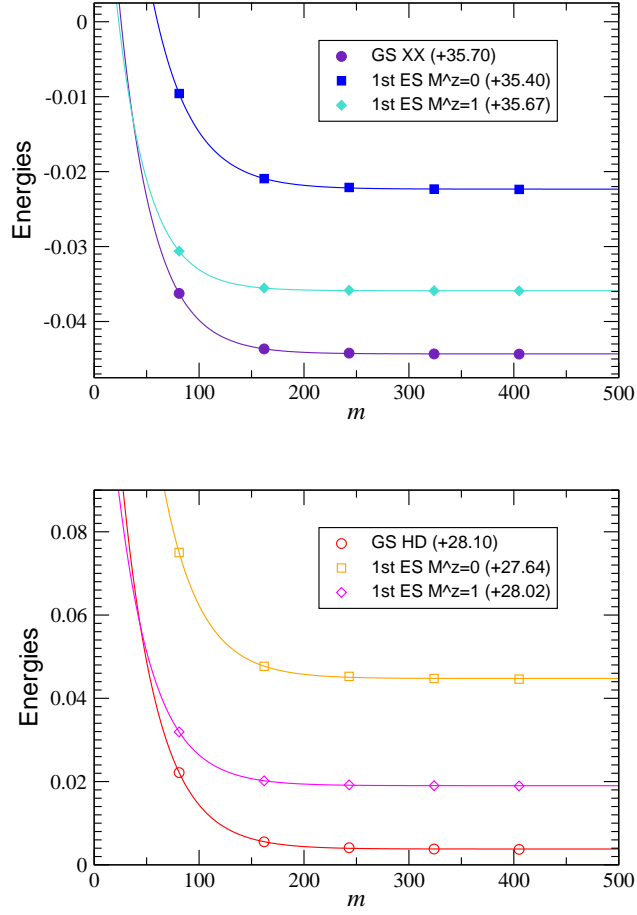


Figure 1: Energies of the GS and of the first excited states within $M^z = 0, 1$ at the points XX and H-D (see text). The symbols represent DMRG values obtained with $L = 32$ and an increasing number of DMRG states (m) while the continuous lines are exponential fits. For clarity reasons, the offsets reported in the legend have been added.

Data Set	M_0
GS XX	16.9 ± 0.4
1st $M^z = 0$	17.6 ± 0.4
1st $M^z = 1$ [†]	15.6 ± 0.4
GS H-D	13.2 ± 0.3
1st $M^z = 0$	15.0 ± 0.2
1st $M^z = 1$ [‡]	11.4 ± 0.3

Table 1: Slopes M_0 of the best fits of the sets plotted in fig. 2 (with same notations). [†] Only with $L \geq 28$; [‡] Only with $L \geq 24$.

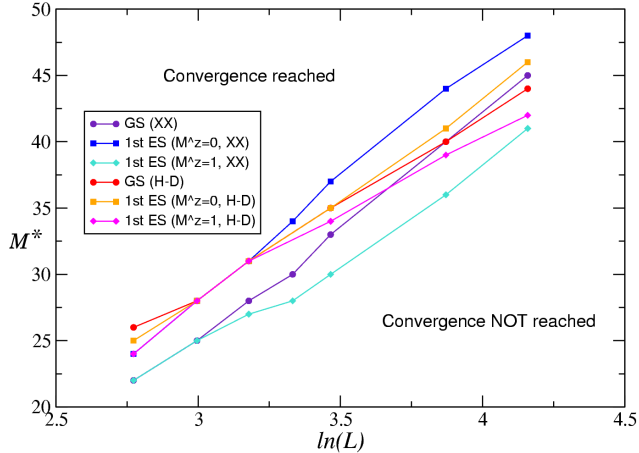


Figure 2: DMRG characteristic length for the points indicated in the legend [XX stands for $(\lambda = 0, D = 0)$ while H-D indicates $(\lambda = 1, D = 0.95)$, close to the Haldane-large- D transition]. The numerical curves separate two regions where the exponential convergence of the low-lying levels with M is essentially reached or not.

we readily get:

$$W_M = \sum_{j>M} Z^j = \frac{Z}{1-Z} Z^M \simeq \frac{\ln L}{\epsilon_0} e^{-\epsilon_0 M / \ln L} . \quad (19)$$

Unfortunately, the effective accuracy gets poorer, by one or two orders of magnitude [3], when we deal with correlation functions. Keeping the errors on the low-lying levels below the desired threshold may not be sufficient so that we had to adopt an additional criterion to decide whether the selected M is large enough or not. In practice, we check systematically the properties of translational and reflectional invariance that we expect from the symmetries of the Hamiltonian. In fact we have observed that one the “symptoms” of a too-small M is the visible (i.e. above numerical uncertainties) lack of some of these invariances. To be more specific, if $C(0, k)$ is a certain correlation function computed starting at $j = 0$, we have always increased M (at the expenses of L) until the bound $|C(L/2, L/2 \pm k) - C(0, k)|/C(0, k) \lesssim 0.05$ was met for k varying from 0 to $L/2$, possibly with the exception of the ranges where $C(0, k)$ is very small, say 10^{-6} . In fig. 3 we give an example with string correlation functions [eq. (18)] at the XX point. These should be translationally invariant but their numerical estimates depend in fact from the starting point j because we have intentionally fixed a too-small value, $M = 50$. It is also interesting to point out that in this example $O_S^x(j, j+r)$ essentially coincides with $(-)^r \langle S_j^x S_{j+r}^x \rangle$ (not plotted). We interpret this coincidence with the onset of planar order at the BKT transition.

5 Examples and Results

The quality of the numerical analysis of the critical properties depends heavily on the location of the critical points of interest. At present, our study focuses primarily on the transitions from the Haldane phase, for which it is convenient to fix some representative values of λ and let D vary across the phase boundaries. This preliminary task of finding $D_c(\lambda)$ turns out to be crucial for subsequent calculations and is divided in two steps.

First, one gets an approximate idea of the transition points using a direct extrapolation in $1/L$ of the numerical values of the gaps, computed at increasing L with

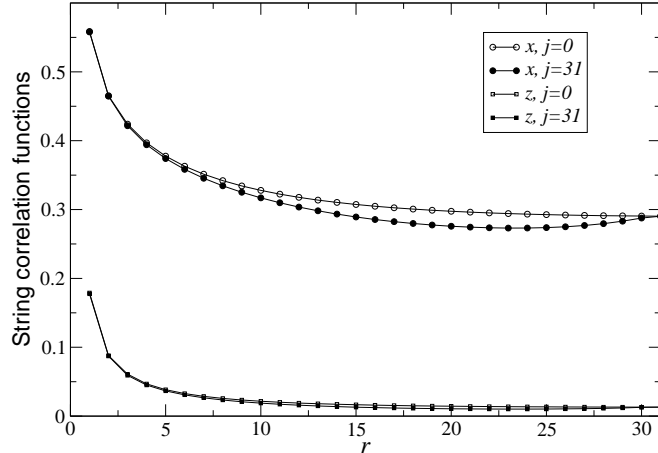


Figure 3: Transverse ($\alpha = x$, circles) and longitudinal ($\alpha = z$, squares) string correlation functions for a chain of 64 sites with PBC at the XX point (see text), computed with only $M = 50$ DMRG states. The empty symbols represent $O_S^\alpha(j = 0, r)$ while the full ones represent $O_S^\alpha(j = 31, 31 + r)$, with an evident dependence on j .

a moderate number of DMRG states. Clearly, one may want to explore a rather large interval of values and so the increments in D will not be particularly small (say 0.1). An example of such a scanning at $\lambda = 0.5$ is presented in fig. 4. Note that at ($\lambda = 0.5, D \simeq 0.6$) one has a first insight on the “cascade” of levels predicted by CFT [eq. (7) for $L \rightarrow \infty$.]

As a second step, the analysis must be refined around the minima of the curves ΔE -vs- D with smaller increments in D and a larger value of M . According to finite-size scaling (FSS) theory ([34] and appendix A), at the true critical point (that is, in the TL) one should see that the data settle to a constant in the log-log plot of the scaled gaps vs L . Fig. 5 shows an example of such an inspection for $\lambda = 0.5$ and D varying about the H-D transition. It is seen that the differences in the slopes of the various curves are not so pronounced. Hence, from this plot we have selected two candidates for the critical point $D_c(0.5)$, namely $D = 0.62$ and $D = 0.65$. At this stage we should mention that in this type of transition also the phenomenological renormalization group (PRG) method [34] typically yields a pair of (pseudo)critical values at fixed L . In this case, these two sequences of values seem to converge to the point $D = 0.62$ (note that in order to see convergence of the curves up to $L = 50$ we had to use 400 DMRG states). Unfortunately, this turns out to be an invalid tie-break because at this point the finite-size β -function increases with increasing L . This is shown in fig. 6, where $\beta_L(0.65)$ is also plotted. The latter scales to zero with a size-dependent slope that we calculate from eq. (24). The extrapolation to $1/L \rightarrow 0$ (and restricted to $L \geq 22$) then gives $\nu = 3.69 \pm 0.04$. As discussed below this is not a particularly good estimate of ν . Nonetheless, the location of the critical point $D_c(0.5) = 0.65$ is quite close to the value $D = 0.635$ obtained in ref. [22] with a method based on twisted boundary conditions and exact diagonalization up to $L = 16$. In this sense, we suspect that the difficulties encountered both with FSS and PRG (roughly speaking, the appearance of “fake” critical points) are due to the peculiar structure of the energy spectrum in this type of transition. In particular, both sides of the transition are massive and it is likely that with PBC we are faced with the scenario proposed by Kitazawa [18]: In eq. (21) the constant C_1 for the first excited state could vanish identically and we have to consider a second-order expansion in $(D - D_c)$. Consequently, the values of

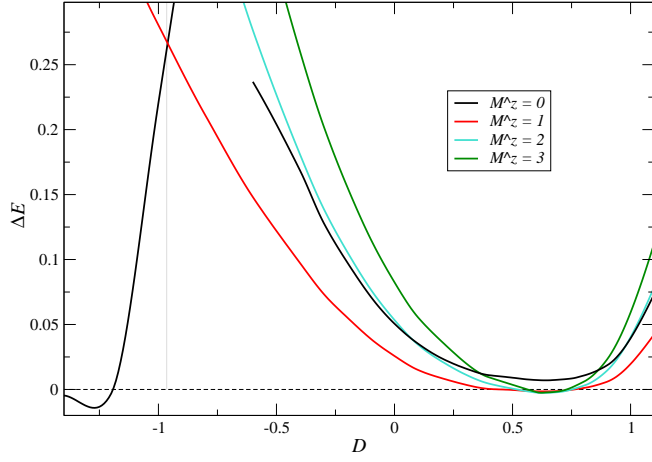


Figure 4: Extrapolations of the gaps between the GS and the first excited states within the indicated sectors of M^z at $\lambda = 0.5$. The values at $L \rightarrow \infty$ have been obtained through a quadratic best fit in $1/L$ from the data at $L = 32, 48, 64, 80$ with 216 DMRG states. For graphical convenience, the various sets have been turned into continuous curves using splines. The vertical gray line indicates the point of intersection between the states with $M^z = 0$ and $M^z = 1$, that is, the analogue of the Haldane triplet at $\lambda = 0.5$.

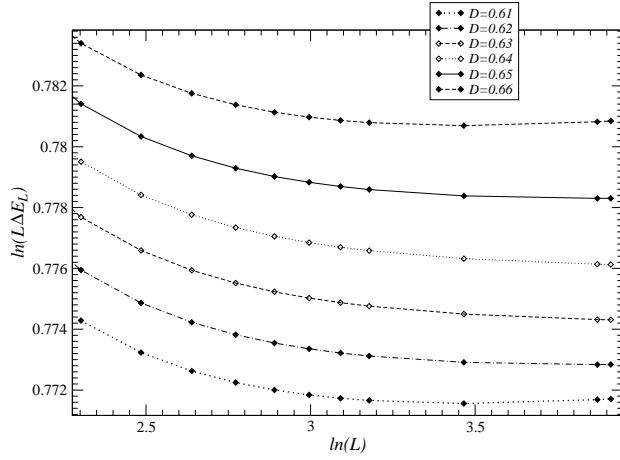


Figure 5: H-D transition at $\lambda = 0.5$: Scaled gap (between $|M^z = 0, b = 0\rangle$ and $|M^z = 1, b = 0\rangle$) at $L = 10, 12, 14, 16, 18, 20, 22, 24, 32, 48, 50$ (with 400 DMRG states), for the values of D indicated in the legend.

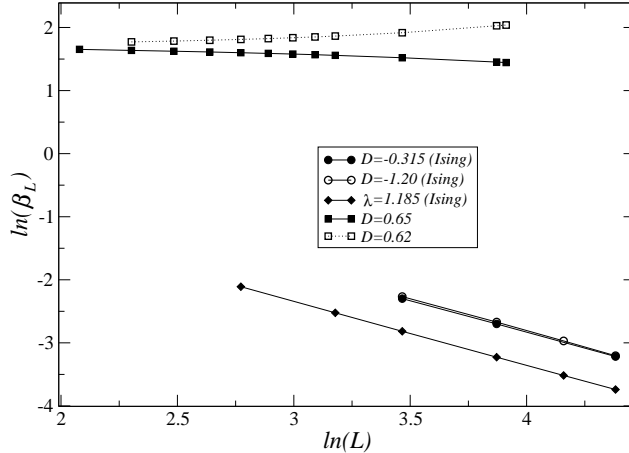


Figure 6: Finite-size β -functions for $(\lambda = 0.5, D = 0.62)$ (open squares), $(\lambda = 0.5, D = 0.65)$ (full squares), $(\lambda = 0.5, D = -1.2)$ (open circles), $(\lambda = 1, D = -0.315)$ (full circles) and $(\lambda = 1.185, D = 0)$ (full diamonds). All the numerical derivatives have been calculated by means of centered differences with $\delta D = 0.01$ for the first two cases (Haldane-large- D transition), $\delta D = 0.005$ for the second two and $\delta\lambda = 0.005$ for the last one. Notice that the three lines for the transitions from the Haldane to the Néel-like phase (Ising type) have essentially the same slope, that is, the same ν .

the critical points are determined via parabolic intersections that are more sensitive to numerical uncertainties. Probably this is also the reason why the scaling analysis of β_L as used here performs poorly. In fact, in our framework the best estimate of ν comes from another method, namely via the scaling dimension of the mass-generating operator. According to the discussion that follows, for $(\lambda = 0.5, D = 0.65)$ we find $\nu = 2.38$, essentially in accord with the values given in [20].

At the transition between the Haldane and the Néel-like phase (henceforth denoted as H-N) these difficulties regarding the location of $D_c(\lambda)$ and the scaling to zero of $\beta_L(D_c)$ are not encountered. For instance, from figs. 4 (left part) and 7 we identify $D_c(0.5) = -1.2$, and it is seen that this value separates between a gapfull phase, where the scaled gap increases with increasing L , and a gapless one (doubly degenerate GS), where it is expected that the scaled gap converges rapidly to zero [19]. Moreover, the pseudo-critical values obtained with the PRG are practically independent of L and coincide with the estimate from FSS. The algebraic decay of $\beta_L(-1.2)$ is rather clear from fig. 6 and one can readily estimate $\nu = 1.023 \pm 0.009$ from the slope of the linear best fit. This is the first hallmark that the H-N transition belongs to the (2D) Ising universality class, as reported by various authors (see below our argument based on the combined use of CFT and DMRG).

Despite some difficulties in locating the critical points (of the H-D line) on the basis of DMRG data, we are now in position to suggest an extension in the usage of this numerical method to approach the critical points of quantum Hamiltonians. Taking advantage of the underlying conformal theory that should be present in all these cases, we focus on the finite-size energy spectrum, as summarized by eqs. (7) and (9). Once the critical point is located, we select a number of states that seem to become degenerate with the GS in the limit $L \rightarrow \infty$. In practice, we consider $\Delta E/2\pi$ and look for straight lines in terms of $1/L$. Then, from a best fit we expect to have a very small offset (ideally a zero gap in the TL) and a slope given by the scaling dimension d_ℓ multiplied by the velocity v . Actually, due to this prefactor we have to

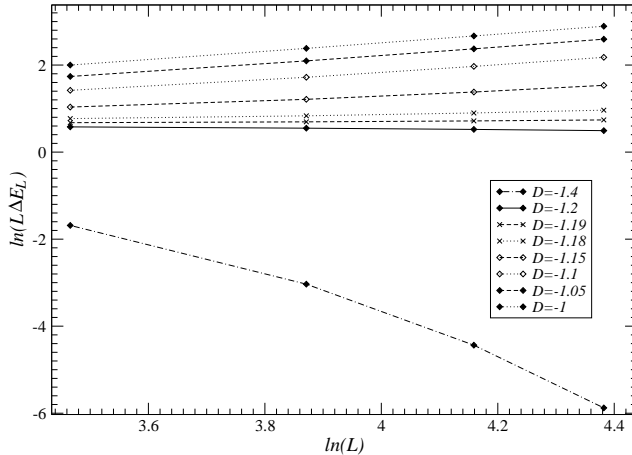


Figure 7: Ising transition at $\lambda = 0.5$: Scaled gap (between $|M^z = 0, b = 0\rangle$ and $|M^z = 0, b = 1\rangle$) at $L = 32, 48, 64, 80$ (with 216 DMRG states), for the values of D indicated in the legend.

imagine a self-consistent procedure: Depending on the type of the transition we have in mind (that is, depending on the conformal anomaly c), we stick on one or more levels in the spectrum that have exactly $d = 1$. Then the slope of these is nothing but v . Once the velocity is estimated, one uses eq. (9) to best fit the product cv and see whether the value of c and the hypothesis on the universality class are self-consistent or not.

To clarify the matter, let us see in detail what happens in the simple case of the H-N transition, that is thought to be in the universality class of the classical 2D Ising model with $c = 1/2$. This can be considered as the paradigm of minimal models in CFT and the corresponding quantum field theory is that of a massless Majorana fermion. Apart from the identity (with zero scaling dimensions) one has only two primary fields with $\Delta_h = 1/16$ and $\Delta_T = 1/2$. In addition, modular invariance demands that the conformal spin ($\Delta - \bar{\Delta}$) of the combinations that enter the partition function (on the torus) must be zero. Hence we are left with two nontrivial primary operators of scaling dimensions $d_T = 1$ and $d_h = 1/8$, that are interpreted as energy and spin density, respectively. The former is responsible for the variations away from the critical temperature and so the correlation length index is given by $\nu = 1/(2 - d_T) = 1$. The latter, from eq. (8), gives the decay exponent of the spin-spin correlation function $\eta_s = 1/4$ at the critical point. At the same time, being $\nu = 1$ [see next eqs. (25) and (26)], one determines also the exponent $\beta = d_h = 1/8$, describing the opening of the magnetization off criticality. Using eq. (9) at the critical point ($\lambda = 0.5, D = -1.2$) we find $\epsilon_\infty = -2.0011961 \pm 0.0000006$ and $cv = 1.222 \pm 0.002$. At this stage we observe a nontrivial feature: The massless modes described by the CFT seem to be all and only the levels within $M^z = 0$, while those with $M^z \neq 0$ maintain a finite energy gap in the TL. Hence, the reference state for the calculation of v will be the second excited state in $M^z = 0$, corresponding to the primary field of conformal dimensions $(1/2, 1/2)$. Using eq. (10) we determine a velocity that extrapolates (quadratically in $1/L$) to $v = 2.44$, so that $c = 0.5008 \pm 0.0008$ and the Ising universality class is confirmed. The scaling dimensions can be estimated from the slopes of the straight lines in a plot like that of fig. 8. In table 2 we compare the theoretical values with the numerical estimates. The overall agreement is good (7 % in the worst case). Only the relevant and marginal cases with $d \leq 2$ are reported. Note that all the marginal operators have nonzero momentum

and so they cannot represent a valid perturbation to the continuum Hamiltonian in as much as they would break translational invariance. The absence of marginal operators suggests that each point of the H-N transition corresponds to the same $c = 1/2$ theory and the line in the phase diagram is “generated” by the mapping from the discrete spin model to the continuum CFT. Repeating the same passages at $\lambda = 1$ we find $D_c(1) = -0.315$, together with $\nu = 2.65$, $\epsilon_\infty = -1.62651$, $c = 0.498 \pm 0.002$ and $\nu = 1.003 \pm 0.006$, as estimated from the decay of $\beta_L(-0.315)$. Notice that in fig. 6 the points ($\lambda = 0.5, D = -1.2$) and ($\lambda = 1, D = -0.315$) have essentially the *same* β -function.

A third case that is worthy of analysis is the λ -driven transition at $D = 0$, that has been recently revisited [5] to argue that it does not belong to the Ising universality class, as it is generally accepted. Taking advantage of previous results, we fixed $D = 0$ in eq. (13) and varied λ about 1.18. From FSS, the best estimate of the critical point is $\lambda_c(0) = 1.185$, in agreement both with [25] and with [5]. From the numerical spectra with $L = 32, 48, 64, 80$ and $M = 300$ we derive $\nu = 2.66$, $\epsilon_\infty = -1.500549 \pm 0.000001$ and $c = 0.503 \pm 0.002$. This value of the central charge, together with estimate $\nu = 0.992 \pm 0.002$ from $\beta_L(1.185)$, leads us to confirm that this transition is in the 2D Ising universality class, as claimed in [25] and refs. therein. As concerns the discrepancy with ref. [5], we should mention that a distinctive point of their analysis is the extrapolation for $M \rightarrow \infty$. On the other hand, we feel that the numerical procedure contains two weak points. First, the conclusion that ν is not sufficiently close to 1, and the consequence that the effective dimensionality is not 2, are drawn from the estimates of the correlation length using a *pure* exponential law that is expected to be true just for an Ising system but is wrong in the deep Haldane phase. According to our experience, having a multi-target code at disposal, it would be better to read the values of ν directly from the excitation gap. The second and more important point is the usage of the infinite-system algorithm. In secs. 1, 3 and 4 we have given indications that this may be a risky procedure if one aims at very precise quantitative results, and that the finite-system algorithm should be preferred (see also refs. [2, 16] regarding this question).

6 Concluding Remarks

The aim of this paper is to give a detailed explanation of the numerical method used to derive the results of ref. [13] and, more generally, to discuss how one can circumvent some of the problems of the DMRG close to criticality. The ideas are explicitly worked out taking some representative point in the $\lambda - D$ phase diagram for the Hamiltonian of eq. (13). In sec. 4 we have argued that close to the transition lines from the Haldane phase (at least the ones with $c = 1$) the convergence is controlled by a characteristic length $L^*(M)$ that appears as a consequence of the truncation to the M states with largest weights in the block density matrix ρ_b . This fact is in line with similar results by other authors [2, 4], and probably lies at the heart of the problem: in the TL the physical system behaves in a critical way but the DMRG procedure introduces a spurious length so that the numerical outcome is no longer scale invariant.

The method that we are suggesting is based on the finite-system DMRG algorithm in order to reduce as much as possible the (environment [2]) errors and has to be applied in an intermediate range of L , not too small so that the signatures of scaling are visible but not too large as compared to $L^*(M)$. Then we make use of powerful finite-size scaling predictions, coming from CFT's, to extract various informations on the effective continuum model, like the “spin velocity” and the central charge, from the spectrum of low-lying excitations. The latter can be computed, within the DMRG, by taking ρ_b as the average of the matrices associated to a given number of excited

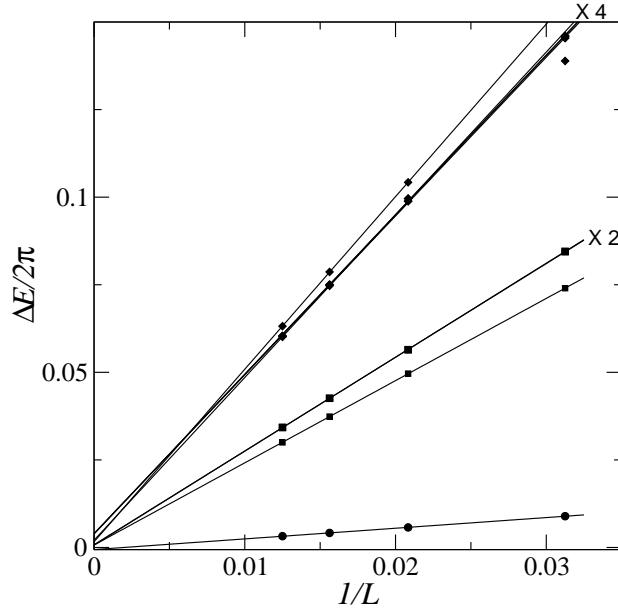


Figure 8: Energy differences, divided by 2π , plotted vs $1/L$ at the Ising transition ($\lambda = 0.5, D = -1.2$). Points represent the numerical values obtained with multi-target DMRG runs ($M = 216$) collecting *nine* excited states within $M^z = 0$. Continuous lines are best-fit whose slopes are given in table 2, together with the theoretical predictions of the scaling dimensions (the labels on the right indicate the multiplicities).

$d_{\text{CFT}} [\times \text{multiplicity}]$	d_{num}	Secondary Indices	Q
0 [$\times 1$]		(0,0)	0
1/8 [$\times 1$]	0.1250 ± 0.0004	(0,0)	0 (or π ?)
1 [$\times 1$]	0.962 ± 0.001	(0,0)	0 (or π ?)
9/8 [$\times 2$]	1.0959 ± 0.0008	(1,0)	$2\pi/L$
	1.100 ± 0.003	(0,1)	$-2\pi/L$
2 [$\times 4$]	1.904 ± 0.004	(2,0)	$4\pi/L$
	1.86 ± 0.01	(0,2)	$-4\pi/L$
	1.87 ± 0.02	(1,0)	$2\pi/L$
	1.87 ± 0.02	(0,1)	$-2\pi/L$

Table 2: Spectrum of conformal dimensions at the Ising transition ($d = d_{\text{primary}} + \text{sec. indices}$). The second column contains the numerical values deduced from fig. 8 using $v = 2.44$. All the multiplicities are met, even if with DMRG calculations only we are not able to classify the four degenerate states in terms of the secondary indices. The fourth column contains the total momentum/conformal spin expected from eq. (5). Question marks indicate that the conformal continuum theory predicts 0 also for those cases that are expected to have $|Q| = \pi$ [19]. We suspect that this is due to the correspondence between the original spin model and the field theory that maps the discrete AFM structure ($|Q| = \pi$) onto the low-momentum sector. Indeed, for the CFT to give $|Q| = \pi$ an extensive secondary index equal to $L/2$ would be needed, and this would yield a nonzero energy gap in the TL.

states that, in turn, are obtained with a thick-restart variant of the Lanczos method (see [28] and sec. 3).

Finally, in sec. 5 we have reported some examples of $c = 1/2$ transitions between the Haldane and the Néel-like phase at large λ . In particular, we have re-examined and confirmed the 2D Ising nature of the critical point at $D = 0$ [25], somehow controverted recently [5].

7 Acknowledgements

We are grateful to L. Campos Venuti, E. Ercolessi, G. Morandi, F. Ravanini, M. Roncaglia and S.-W. Tsai for their useful interventions during the preparation of the paper. This work was partially funded by the Italian MIUR, through the COFIN project entitled “Sistemi Elettronici e di Spin in Bassa Dimensionalità: Teorie di Campo, Integrabilità e Metodi Numerici”.

A Appendix: Brief Survey of FSS Theory

Ideally, we should locate the critical points of a quantum system by looking at the smallest energy gap, ΔE , as a function of a (relevant) parameter g and identify g_c through the condition $\Delta E(g_c) = 0$. For an algebraic transition the critical index ν controls the opening of the gap, $\Delta E \propto |g - g_c|^\nu$. However, when the critical point is approached numerically we encounter two related problems. First, the system’s size is necessarily finite and a true phase transition is forbidden. Second, if we are able to deal with sufficiently large systems close to g_c , the energy gap may become so small to be comparable with the errors introduced by the algorithm (or, ultimately, by the machine). Hence we need a prescription to infer the location of the critical point from nonzero values of ΔE_L at finite L .

In FSS theory [35, 20, 34] one usually invokes the following ansatz (quantum Hamiltonian notations):

$$\Delta E_L = \frac{1}{L} F(\zeta), \quad \zeta \equiv L^{1/\nu} |g - g_c|, \quad (20)$$

so that the scaling variable ζ covers these two regimes

- (a) $\zeta \rightarrow 0$ for $g \rightarrow g_c$ at fixed L . In this regime we should see a finite system at the infinite-size critical point. Since ΔE_L is in fact an inverse correlation length ξ_L , we expect the latter to be as large as possible, that is to say $\Delta E_L \propto L^{-1}$. Compatibility with eq. (20) then requires $F(0) \neq 0$. This is exactly the case for which the continuum description of conformal field theories applies (sec. 2). In particular, the first terms of eq. (12) should be nothing but a McLaurin series of $F(\zeta)$ for $\zeta \ll 1$:

$$\Delta E_L = \frac{2\pi\nu}{L} [(2 - \nu^{-1}) + C_1\zeta + C_2\zeta^2 + \dots], \quad (21)$$

because we have identified V with the relevant operator that opens the gap, and in this case $d_V = 2 - \nu^{-1}$.

- (b) $\zeta \rightarrow \infty$, which means $(L/\xi_L)^{1/\nu} \gg 1$. This regime mimics the TL, in the sense that ξ_L is large but finite because the system is slightly off-critical and L is sufficiently large so that scaling laws appear. Hence L must effectively cancel in eq. (20), leaving just $|g - g_c|^\nu$. This is possible if:

$$F(\zeta) \sim \zeta^\nu \quad \zeta \gg 1. \quad (22)$$

From (a) we derive the way to locate the critical points through FSS: Plot $\ln(\Delta E_L)$ vs $\ln L$ and look for the value of g that best gives a straight line with slope -1 . Actually, we can be even more severe looking for slope 0 in the curves of the scaled gaps $L\Delta E_L$. As far as the index ν is concerned, one may consider the finite-size β -function, $\beta_L^{-1}(g) \equiv \partial \ln(\Delta E_L)/\partial g$, evaluated at $g = g_c$ as determined above (apart from the sign):

$$\beta_L(g_c) = [F(\zeta)/F'(\zeta)]_{\zeta=0} L^{-1/\nu}, \quad (23)$$

where F' denotes the derivative with respect to ζ and $F'(0)$ is also assumed to be nonzero. In principle $\beta_L(g_c)$ should vanish with an exponent $1/\nu$ that represents the asymptotic slope in log-log scales. Alternatively, since the scaling region may be reachable only for very large L , one can calculate the discrete logarithmic derivative through a size increment $L \rightarrow L + \delta L$:

$$\frac{1}{\nu_L} \equiv -\frac{\ln \beta_{L+\delta L}(g_c) - \ln \beta_L(g_c)}{\ln(L + \delta L) - \ln L}, \quad (24)$$

and this should converge to $1/\nu$ when $L \rightarrow \infty$.

Finally, the ansatz (20) can be generalized to other physical quantities that behave as $\mathcal{Q}(g) \propto |g - g_c|^{\nu_{\mathcal{Q}}}$ near the critical point:

$$\mathcal{Q}_L(g) = L^{-z_{\mathcal{Q}}} F_{\mathcal{Q}}(\zeta), \quad (25)$$

with the same scaling variable ζ and scaling exponent $z_{\mathcal{Q}}$. As above, in the critical regime (a) $\zeta \rightarrow 0$ we shall require $F_{\mathcal{Q}}(0) \neq 0$, while in the off-critical regime (b) the scaling exponent $\nu_{\mathcal{Q}}$ emerges provided that $F_{\mathcal{Q}} \sim \zeta^{\nu_{\mathcal{Q}}}$ for $\zeta \rightarrow \infty$, and $z_{\mathcal{Q}} = \nu_{\mathcal{Q}}/\nu$. In many cases, \mathcal{Q}^2 is a squared order parameter given by the asymptotic value of a certain correlation function, $\langle O_{\mathcal{Q}}(0)O_{\mathcal{Q}}(r) \rangle$, that slightly off the critical point behaves as:

$$\langle O_{\mathcal{Q}}(0)O_{\mathcal{Q}}(r) \rangle \propto \frac{G_{\mathcal{Q}}(r/\xi)}{r^{2d_{\mathcal{Q}}}}, \quad (26)$$

$d_{\mathcal{Q}}$ being the scaling dimension of $O_{\mathcal{Q}}$. At this stage we can parallel the scaling argument of Ginsparg (sec. 5.1 of [12]) evaluating eq. (26) just at the correlation length itself, $r = \xi \propto |g - g_c|^{-\nu}$ thereby having $\langle O_{\mathcal{Q}}(0)O_{\mathcal{Q}}(\xi) \rangle \sim \mathcal{Q}^2 \sim G_{\mathcal{Q}}(1)|g - g_c|^{2\nu d_{\mathcal{Q}}}$. Hence we find the scaling law $d_{\mathcal{Q}} = \nu_{\mathcal{Q}}/\nu$, that tells that $z_{\mathcal{Q}}$ in eq. (25) is nothing but the scaling dimension of the operator associated to the order parameter \mathcal{Q} . In ref. [13] we have used this property to derive the decay exponents of ordinary (transverse channel) and string (z -channel) correlation functions in $c = 1$ phases by applying eq. (25) to the corresponding Néel and string order parameters evaluated at half chain.

References

- [1] For an introduction and a series of applications of the DMRG see: I. Peschel, X. Wang, M. Kaulke and K. Hallberg (editors), *Density-Matrix Renormalization - A New Numerical Method in Physics* (Berlin, Springer, 1999).
- [2] Ö. Legeza and G. Fáth, Phys. Rev. B **53**, 14349 (1996).
- [3] Ö. Legeza, J. Röder and B. A. Hess, Phys. Rev. B **67**, 125114 (2003).
- [4] M. Andersson, M. Boman and S. Östlund, Phys. Rev. B **59**, 10493 (1999).
- [5] M. Capone, S. Caprara and L. Cataldi, *Quantum phase transition in easy-axis antiferromagnetic integer-spin chains*, e-print at <http://arxiv.org/abs/cond-mat/0307266>.
- [6] J. B. Kogut, Rev. Mod. Phys. **51**, 659 (1979).
- [7] A. B. Zamolodchikov and V. Fateev, Sov. J. Nucl. Phys. **32**, 298 (1980).

- [8] I. Peschel, M. Kaulke and Ö. Legeza, *Ann. Phys. (Leipzig)* **8**, 153 (1999).
- [9] K. Okunishi, Y. Hieida and Y. Akutsu, *Phys. Rev. E* **59**, R6227 (1999).
- [10] P. Di Francesco, P. Mathieu and D. Senechal, *Conformal Field Theory* (New York etc., Springer, 1997).
- [11] F. Ravanini, *Finite Size Effects in Integrable Quantum Field Theory*, e-print at <http://arxiv.org/abs/hep-th/0102148>.
- [12] P. Ginsparg in *Fields, Strings and Critical Phenomena: Les Houches 1988, Session XLIX*, edited by E. Brézin and J. Zinn-Justin (Amsterdam etc., North-Holland, 1990).
- [13] C. Degli Esposti Boschi, E. Ercolessi, F. Ortolani and M. Roncaglia, *Eur. Phys. J. B* **35**, 465 (2003).
- [14] H. W. J. Blöte, J. L. Cardy and M. P. Nightingale, *Phys. Rev. Lett.* **56**, 742 (1986).
- [15] I. Affleck, *Phys. Rev. Lett.* **56**, 746 (1986).
- [16] S.-W. Tsai and J. B. Marston, *Phys. Rev. B* **62**, 5546 (2000).
- [17] J. L. Cardy, *Nucl. Phys. B* **270** [FS16], 186 (1986).
- [18] A. Kitazawa, *J. Phys. A: Math. Gen.* **30**, L285 (1997).
- [19] R. Botet, R. Jullien and M. Kolb, *Phys. Rev. B* **28**, 3914 (1983).
- [20] U. Glaus and T. Schneider, *Phys. Rev. B* **30**, 215 (1984).
- [21] H. J. Schulz, *Phys. Rev. B* **34**, 6372 (1986).
- [22] W. Chen, K. Hida and B. C. Sanctuary, *Phys. Rev. B* **67**, 104401 (2003).
- [23] S. R. White, *Phys. Rev. Lett.* **69**, 2863 (1992).
- [24] S. R. White, *Phys. Rev. B* **48**, 10345 (1993).
- [25] A. Kitazawa and K. Nomura, *J. Phys. Soc. Japan* **66** 3944 (1997).
- [26] W. Chen, K. Hida and B. C. Sanctuary, *J. Phys. Soc. Japan* **69**, 237 (2000).
- [27] T. Kennedy and H. Tasaki, *Commun. Math. Phys.* **147**, 431 (1992).
- [28] K. Wu and H. Simon, *SIAM J. Matrix Anal. Appl.* **22**, 602 (2000).
- [29] S. R. White and R. L. Martin, *J. Chem. Phys.* **110**, 4127 (1999).
- [30] M. C. Chung and I. Peschel, *Phys. Rev. B* **64**, 064412 (2001).
- [31] F. D. M. Haldane, *Phys. Rev. Lett.* **50**, 1153 (1983).
- [32] M. den Nijs and K. Rommelse, *Phys. Rev. B* **40**, 4709 (1989).
- [33] R. Jullien and P. Pfeuty, *J. Phys. A: Math. Gen.* **14**, 3111 (1981).
- [34] C. J. Hamer and M. N. Barber, *J. Phys. A: Math. Gen.* **14**, 241 (1981).
- [35] M. E. Fisher and M. N. Barber, *Phys. Rev. Lett* **28**, 1516 (1972).